Structure of saddle-node and cusp bifurcations of periodic orbits near a non-transversal T-point

Antonio Algaba, Fernando Fernández-Sánchez, Manuel Merino, Alejandro J. Rodríguez-Luis

NODY9815_source.tex, 20/08/2010, 9:09 p. 1

Nonlinear Dynamics manuscript No.
(will be inserted by the editor)

Structure of saddle-node and cusp bifurcations of periodic orbits near a non-transversal T-point

Antonio Algaba · Fernando Fernández-Sánchez · Manuel Merino · Alejandro J. Rodríguez-Luis

Received: date / Accepted: date

Abstract Non-transversal T-points have been recently found in problems from many different fields: electronic circuits, pendula and laser problems. In this work we study a model, based on the construction of a Poincaré map, that describes the behaviour of curves of saddle-node and cusp bifurcations in the vicinity of such a non-transversal T-point. This model is also able to predict, reproduce and explain the numerical results previously obtained in Chua's equation.

Keywords Periodic Orbits · Cusp bifurcation · Saddle-node · T-point · Global bifurcations

1 Introduction

An important task for the understanding of the dynamics of parameterized systems of autonomous ordinary differential equations is the determination of the organizing centres as well as the bifurcations they exhibit (see, for instance, [18, 24, 27, 31] as general references). Where a complex bifurcation scenario exists, a combination of analytical and numerical tools is usually needed. Thus, to complement theoretical results, numerical continuation can be carried out in one parameter (bifurcation diagrams such as period versus parameter) or in two (or more) parameters (bifurcation sets, loci where bifurcations occur in the parameter space).

When this continuation is performed, one can sometimes find closed curves. For instance, the presence of isolas (isolated closed curves) in bifurcation diagrams of periodic orbits has been detected in relation to Hopf curves [11]. The appearance of an isola configuration depends on the choice of the bifurcation parameter as well as on the shape of the bifurcation curve.

A typical o-shaped isola of periodic orbits appears when moving inside resonance zones close to the tip where the corresponding Arnold's tongues emerge (see, for instance, Fig. 12(a) in [1]).

Another kind of isola of a certain type of periodic orbit was detected in an electronic circuit [13]. In that work, the mechanism of their formation is shown and their existence is related to cusp bifurcations and to Shil'nikov homoclinic connections.

In other works, certain types of isola are organized by homoclinic bifurcations/tangencies. In this way, it has been shown that primary periodic orbits lie on an infinity of isolas in a neighbourhood of a homoclinic tangency to a periodic orbit [19]. Also finitely and infinitely many isolas of periodic orbits have been found, unfolding a non-transverse Shil'nikov-Hopf bifurcation [10].

The existence of closed curves of global bifurcations (homoclinic and heteroclinic connections) in Chua's equation [28] has been reported numerically [4]. The mechanism of formation/destruction on such curves, when a third parameter is moved, is also qualitatively described and is related to a failure of transversality of a curve of T-points in a three-dimensional parameter space. This

We would like to thank the reviewers for their useful comments and suggestions. This work has been partially supported by the *Ministerio de Educación y Ciencia, Plan Nacional I+D+I* co-financed with FEDER funds, in the frame of the project MTM2007-64193 and by the *Consejería de Educación y Ciencia de la Junta de Andalucía* (FQM-276, TIC-0130 and P08-FQM-03770).

A. Algaba, M. Merino
Dept. Mathematics, Fac. Ciencias Experimentales, Univ. Huelva
Avda. Tres de Marzo s/n, 21071 Huelva, Spain.
E-mail: algaba@uhu.es, merino@uhu.es

F. Fernández-Sánchez, A. J. Rodríguez-Luis
Dept. Applied Mathematics II, E.S. Ingenieros, Univ. Sevilla
Camino de los Descubrimientos s/n, 41092 Sevilla, Spain.
E-mail: fefesan@us.es, ajrluis@us.es

curve emerged from a triple-zero linear degeneracy of the equilibrium at the origin [3]. The set of curves of saddle-node bifurcations of periodic orbits related to the closed curves of global bifurcations in Chua's equation has been also numerically studied [5].

On the other hand, T-points are codimension-two organizing centres of global bifurcations and complex periodic behaviour in, at least, three-dimensional systems. Among others, references [16, 8, 14] have been devoted to obtaining different models, based on Poincaré maps, to study T-points and the global bifurcations that such points organize in the parameter plane. These models are valid for values of the parameters close to the T-point. Specifically, if the two involved equilibria are saddle-foci, two spiral curves, corresponding to homoclinic connections to both equilibria, and a double infinity of spiral curves of saddle-node bifurcations of periodic orbits emerge from such a T-point.

In the case of reversible systems, bifurcations of periodic orbits are also analyzed using Poincaré maps [25]. Different techniques based on Lin's method [26] are also used in [21] to study complex behaviour in a neighbourhood of a T-point.

Here we investigate what happens with the curves of saddle-node bifurcations of periodic orbits in the presence of a failure of transversality in a curve of T-points. That is, the sequence of bifurcation planes obtained by moving a third parameter shows an interaction between two T-points that collapse and disappear for certain values of the parameters. As a consequence, the curves of bifurcations of periodic orbits organized by each T-point are bound to interact and new behaviour is expected.

To be precise, while the shape of the different curves of global bifurcations can be directly predicted from the previous models [16, 8, 14] when the parameters are close to each T-point, far from them the models fail. Thus, to analyse the corresponding system, it is necessary to build another model which collects all this new behaviour. The idea is to construct a new Poincaré map that will be valid for values of the parameters close to that where the two T-points collapse. This point in the parameter space, obtained from a non-transversal intersection between a curve of T-points and a parameter plane, will be denoted as *non-transversal T-point*, in order to simplify the notation.

These kinds of bifurcations have been found in systems that appear from different fields: Chua's equation [4], a modified van der Pol-Duffing electronic oscillator [2], an inverted pendulum with delayed feedback control [23], a model for solitary pulses in an excitable reaction-diffusion medium [20] and several models related to lasers (see [30, 22] and the references therein).

In [22], the failure of transversality in the T-points curve (called *codimension-two-plus-one event* in [30]) is physically relevant in the model analyzed. In fact, closed curves of homoclinic connections are indeed found numerically in a neighbourhood of such a point. This agrees with the theoretical results obtained in [2] and confirmed numerically in Chua's equation [4].

Another interesting work that provides some theoretical analysis related to [22] by constructing Poincaré maps is [9].

In [30], authors raise the need to perform a detailed study, from the bifurcations theory point of view, of the non-transversal T-point. In this work we partially answer the question concerning the structure of the periodic orbits and their degeneracies in a neighbourhood of such a point. Thus, we extend the theoretical study of homoclinic connections performed in [2] and, at the same time, we theoretically confirm the numerical results on saddle-node bifurcation curves obtained in Chua's equation [5].

This paper is organized as follows. In Sect. 2 we describe the model derived in [2]. Sect. 3, the core of the paper, is devoted to the analysis of the model: for the principal periodic orbits (Sect. 3.1), for their saddle-node bifurcations (Sect. 3.2) and for cusp bifurcations (Sect. 3.3). This section is concluded with a numerical study of the model (Sect. 3.4) and the explanation, in terms of the singularity theory, of some found behaviour (Sect. 3.5). We finish the paper with some conclusions.

2 Derivation of the model: global bifurcations

The model we use to analyze the failure of transversality of a curve of T-points has been obtained in a previous work [2] and it is based on Poincaré maps (see, for instance, [16, 8, 14]. Since this model is going to be used in the analysis of periodic orbits we now briefly outline the principal steps of its derivation although we refer the reader to [2] for more details about the construction procedure and the validity of the equations.

Let us assume that, in a neighbourhood of the origin in the parameter space where a non-transversal T-point appears, the system under study has, at least, two saddle-focus equilibria, Q_1 and Q_2. Let us also assume that the equilibrium Q_1 has a one-dimensional unstable manifold and a two-dimensional stable one, whereas Q_2 has a two-dimensional unstable manifold and a one-dimensional stable one. For the values of the parameters where a T-point exists, the equilibria are connected in the following way: the one-dimensional unstable manifold of Q_1 and the one-dimensional stable manifold of Q_2 coincide, while the two-dimensional stable manifold

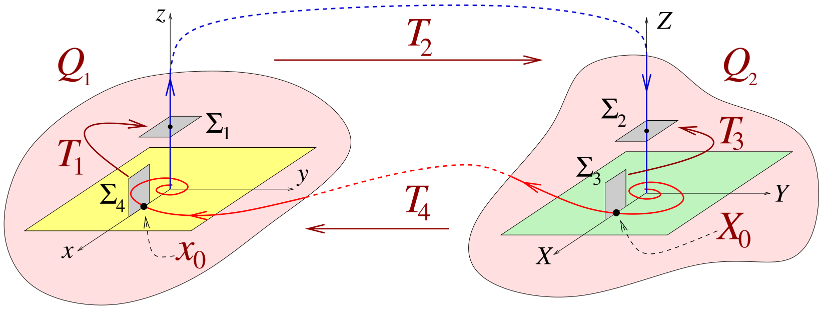

Fig. 1 Schematic diagram of the heteroclinic T-point cycle in the three-dimensional phase space

of Q_1 and the unstable one of Q_2 have, at least, one transversal intersection, which we will name *the closing orbit* (see Fig. 1).

First we choose appropriate coordinates (x, y, z) and (X, Y, Z) such that the system can be written as

$$\begin{cases} \dot{x} = -px - \omega y, \\ \dot{y} = \omega x - py, \\ \dot{z} = \lambda z, \end{cases} \quad \text{or} \quad \begin{cases} \dot{X} = PX - \Omega Y, \\ \dot{Y} = \Omega X + PY, \\ \dot{Z} = -\Lambda Z, \end{cases} \tag{1}$$

in a neighbourhood of the equilibrium Q_1 or, respectively, Q_2 [16,8,14]. Parameters Λ, λ, P and p are positive while Ω and ω do not vanish.

Using these new coordinates, four cross-sections Σ_i can be considered:

$$\Sigma_1 = \{(x, y, z);\ z = h\},$$
$$\Sigma_2 = \{(X, Y, Z);\ Z = H\},$$
$$\Sigma_3 = \{(X, Y, Z);\ Y = 0,\ H \geq Z > 0\},$$
$$\Sigma_4 = \{(x, y, z);\ y = 0,\ h \geq z > 0\},$$

where h and H are small positive numbers. We also choose two points of the closing orbit, $(X_0, 0, 0) \in \Sigma_3$ and $(x_0, 0, 0) \in \Sigma_4$.

Taking into account that the four cross-sections Σ_1, Σ_2, Σ_3 and Σ_4 are transversal to the flow in small neighbourhoods of $(0, 0, h)$, $(0, 0, H)$, $(X_0, 0, 0)$ and $(x_0, 0, 0)$ respectively, it is possible to obtain the equations of the partial maps between the cross-sections:

- $T_1 : \Sigma_4 \to \Sigma_1$ is given by $T_1(x, 0, z) = (x', y', h)$, where
$$\begin{pmatrix} x' \\ y' \end{pmatrix} = \begin{pmatrix} xz^\delta h^{-\delta} \cos(\theta \log z + \phi) \\ xz^\delta h^{-\delta} \sin(\theta \log z + \phi) \end{pmatrix},$$
$\delta = p/\lambda$, $\theta = -\omega/\lambda$, $\phi = (\omega/\lambda) \log h$.
- $T_2 : \Sigma_1 \to \Sigma_2$ is given by $T_2(x', y', 0) = (X', Y', 0)$ where
$$\begin{pmatrix} X' \\ Y' \end{pmatrix} = \begin{pmatrix} d_1 \\ d_2^2 - \mu \end{pmatrix} + \begin{pmatrix} a & b \\ c & d \end{pmatrix} \begin{pmatrix} x' \\ y' \end{pmatrix},$$
with $ad - bc \neq 0$.
- $T_3 : \Sigma_3 \to \Sigma_2$ is given by $T_3(X, 0, Z) = (X', Y', H)$, where
$$\begin{pmatrix} X' \\ Y' \end{pmatrix} = \begin{pmatrix} XZ^\Delta H^{-\Delta} \cos(\Theta \log Z + \Phi) \\ XZ^\Delta H^{-\Delta} \sin(\Theta \log Z + \Phi) \end{pmatrix},$$
$\Delta = P/\Lambda$, $\Theta = \Omega/\Lambda$ and $\Phi = (-\Omega/\Lambda) \log H$.
- $T_4 : \Sigma_3 \to \Sigma_4$ is given by $T_4(X, 0, Z) = (x, 0, z)$ where
$$\begin{pmatrix} x \\ z \end{pmatrix} = \begin{pmatrix} x_0 \\ 0 \end{pmatrix} + \begin{pmatrix} A & B \\ C & D \end{pmatrix} \begin{pmatrix} X - X_0 \\ Z \end{pmatrix},$$
with $AD - BC \neq 0$ and $C \neq 0$.

From now on parameters d_1, d_2 and μ (given in T_2) act as unfolding parameters of the non-transversal T-point. Moreover, they can be assumed, as in [14], to be independent of the other parameters $\delta, \Delta, \theta, \Theta, \ldots$

The model described above was used in [2] to study the global bifurcations organized by the non-transversal T-point in a neighbourhood of the origin in the parameter space. The first result given in [2] states that there exists a curve of T-points given by equations $d_1 = 0$, $\mu = d_2^2$. In fact, the non-transversal T-point is located at the origin of the parameter space.

Equations for surfaces of homoclinic orbits to Q_1 organized by the non-transversal T-point were also given in [2]:

$$\begin{pmatrix} d_1 \\ d_2 \end{pmatrix} \tag{2}$$
$$= \begin{pmatrix} (X_0 - \frac{D}{C} Z) Z^\Delta H^{-\Delta} \cos(\Theta \log Z + \Phi) \\ \pm\sqrt{\mu + (X_0 - \frac{D}{C} Z) Z^\Delta H^{-\Delta} \sin(\Theta \log Z + \Phi)} \end{pmatrix}.$$

It is obvious that the existence of curves of homoclinic orbits to Q_1 in the plane (d_1, d_2), for different values of μ, is determined by the sign of the argument of the square root

$$f(Z) = \mu + \left(X_0 - \frac{D}{C} Z\right) Z^\Delta H^{-\Delta} \sin(\Theta \log Z + \Phi).$$

The results obtained from the analysis of this square root are summarized in another theorem in [2].

Equations for surfaces of homoclinic orbits to Q_2 organized by the non-transversal T-point, can be found in a similar way:

$$\begin{pmatrix} d_1 \\ d_2 \end{pmatrix} = \begin{pmatrix} -[x_0 + (A/C)z]z^{\delta}h^{-\delta} \\ \pm\left(\mu - [x_0 + (A/C)z]z^{\delta}h^{-\delta} \right. \\ \times [a\cos(\theta\log z + \phi) + b\sin(\theta\log z + \phi)] \\ \left. \times [a\cos(\theta\log z + \phi) + b\sin(\theta\log z + \phi)]\right)^{1/2} \end{pmatrix}. \tag{3}$$

3 Analysis of the model: principal periodic orbits and their bifurcations

The excellent results obtained in [2] for the homoclinic connections to the equilibrium Q_1 are a good reason to analyze bifurcations of periodic orbits using the same first-order model. Moreover, the results in [2] could be expected, in a certain way, because the surface of homoclinic connections around the curve of T-points, in the three-dimensional parameter space, has a "simple" structure. Let us describe roughly this structure: if the curve of T-points were a straight line we could think of the surface of homoclinic connections as a spiral cylinder around it; folding the curve of T-points the surface folds in the same way (see Fig. 2). The curves obtained from the intersections between this surface and the parallel sections for fixed values of μ are easily visualized and correspond to those shown in [2].

On the contrary, the surfaces, curves or points of bifurcations of periodic orbits (fold, period doubling, etc.) cannot be easily imagined, even using a similar reasoning to that used for homoclinic connections. Thus, a good test for the model is the comparison between the results that can be derived from it, about bifurcations of periodic orbits, and numerical calculations obtained for Chua's equation [5].

3.1 Principal periodic orbits

A T-point heteroclinic cycle organizes a rich structure of periodic orbits. This work deals with a particular type of these orbits (see Fig. 3). They can be called *principal* periodic orbits and correspond to the fixed points of the map $T_2 \circ T_1 \circ T_4 \circ T_3^{-1}$ or, in other way, to the solutions $(X, 0, Z)$ to the system $T_2(T_1(T_4(Z))) = T_3(Z)$.

Thus, let us consider a point $(X, 0, Z) \in \Sigma_3$ belonging to a periodic orbit. From the equations of T_4 it is possible to obtain x and X in terms of z and Z:

$$x = x_0 + \frac{1}{C}(Az + (BC - AD)Z),$$
$$X = X_0 + \frac{1}{C}(z - DZ).$$

So, the point $(X, 0, Z)$ is mapped, under T_4, into a point

$$(x_0 + \frac{1}{C}(Az + (BC - AD)Z), 0, z) \in \Sigma_4.$$

Now, mapping this point under T_1 we obtain a point $(x', y', h) \in \Sigma_1$, where

$$\begin{pmatrix} x' \\ y' \end{pmatrix} = [x_0 + \frac{1}{C}(Az + (BC - AD)Z)]z^{\delta}h^{-\delta} \times \begin{pmatrix} \cos(\theta\log z + \phi) \\ \sin(\theta\log z + \phi) \end{pmatrix}. \tag{4}$$

The image under T_2 is a point $(X', Y', H) \in \Sigma_2$ such that

$$\begin{pmatrix} X' \\ Y' \end{pmatrix} = \begin{pmatrix} d_1 \\ d_2^2 - \mu \end{pmatrix} + [x_0 + \frac{1}{C}(Az + (BC - AD)Z)]z^{\delta}h^{-\delta} \times \begin{pmatrix} a & b \\ c & d \end{pmatrix} \begin{pmatrix} \cos(\theta\log z + \phi) \\ \sin(\theta\log z + \phi) \end{pmatrix}. \tag{5}$$

On the other hand, mapping $(X, 0, Z) = (X_0 + \frac{1}{C}(z - DZ), 0, Z)$ by T_3, we obtain the point $(X', Y', H) \in \Sigma_2$ where

$$\begin{pmatrix} X' \\ Y' \end{pmatrix} = [X_0 + \frac{1}{C}(z - DZ)] \times Z^{\Delta}H^{-\Delta} \begin{pmatrix} \cos(\Theta\log Z + \Phi) \\ \sin(\Theta\log Z + \Phi) \end{pmatrix}. \tag{6}$$

From Eqs. (5) and (6) we have two different expressions for X' and Y'. The system will have a periodic orbit if both expressions coincide. This reasoning proves the following theorem:

Theorem 1 *Fixing a point (d_1, d_2, μ) in the parameter space, a principal periodic orbit of the system has to intersect Σ_3 and Σ_4, respectively, in two points $(X, 0, Z)$ and $(x, 0, z)$, where*

$$x = x_0 + \frac{1}{C}(Az + (BC - AD)Z),$$
$$X = X_0 + \frac{1}{C}(z - DZ), \tag{7}$$

and

$$\begin{pmatrix} d_1 \\ d_2^2 - \mu \end{pmatrix} = [X_0 + \frac{1}{C}(z - DZ)] \times Z^{\Delta}H^{-\Delta} \begin{pmatrix} \cos(\Theta\log Z + \Phi) \\ \sin(\Theta\log Z + \Phi) \end{pmatrix} - [x_0 + \frac{1}{C}(Az + (BC - AD)Z)] \times z^{\delta}h^{-\delta} \begin{pmatrix} a & b \\ c & d \end{pmatrix} \begin{pmatrix} \cos(\theta\log z + \phi) \\ \sin(\theta\log z + \phi) \end{pmatrix}. \tag{8}$$

System (8) is a relationship between the principal parameters (d_1, d_2, μ) and the variables z and Z. From any solution (z, Z, d_1, d_2, μ) of Eq. (8), the other coordinates $(x,\ X,\ \ldots)$ of the intersections between the

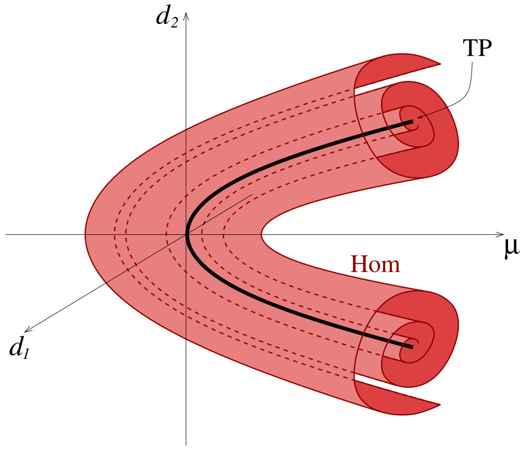

Fig. 2 Surface of homoclinic orbits to Q_1, HO, in the parameter space (d_1, d_2, μ), around the curve of T-points, TP.

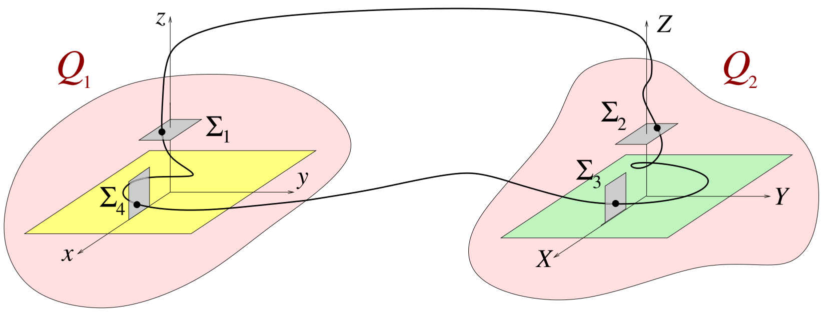

Fig. 3 Periodic orbit related to the T-point

periodic orbit and the transversal sections to the flow can be obtained using Eqs. (4), (5) and (7).

A first way to understand system (8) is to analyze its solutions close to the curves of homoclinic connections [15]; in fact, the equations for these global connections, (2) and (3), can be recognized as terms of Eq. (8). We select the curve of homoclinic connections to Q_1 and a similar reasoning will be valid for the curve of homoclinic connections to Q_2.

Thus, let us assume that μ is fixed and consider a point $\bar{P} = (\bar{d_1}, \bar{d_2})$ of the curve of homoclinic connections to Q_1, with $\bar{d_2} > 0$ (the negative case is analogous and the zero value will be considered below). From Eq. (2) it corresponds to a certain positive value $Z = \bar{Z}$. When this value is fixed in Eq. (8), a curve of periodic orbits, parameterized by z, is obtained at the (d_1, d_2)-plane:

$$\begin{aligned}\begin{pmatrix} d_1 \\ d_2^2 \end{pmatrix} &= \begin{pmatrix} 0 \\ \mu \end{pmatrix} + [X_0 + \frac{1}{C}(z - D\bar{Z})] \\ &\quad \times \bar{Z}^{\Delta} H^{-\Delta} \begin{pmatrix} \cos\left(\Theta \log \bar{Z} + \Phi\right) \\ \sin\left(\Theta \log \bar{Z} + \Phi\right) \end{pmatrix} \\ &\quad - [x_0 + \frac{1}{C}(Az + (BC - AD)\bar{Z})] \\ &\quad \times z^{\delta} h^{-\delta} \begin{pmatrix} a & b \\ c & d \end{pmatrix} \begin{pmatrix} \cos\left(\theta \log z + \phi\right) \\ \sin\left(\theta \log z + \phi\right) \end{pmatrix}.\end{aligned} \tag{9}$$

Note that, in order to get simplified equations, we have shown the second equation for d_2^2 instead of d_2. In any case, as $\bar{d_2}$ is positive, we only consider the positive branch of the corresponding square root.

Several conclusions are inferred from a first study of Eq. (9). Obviously the curve tends to $\bar{P} = (\bar{d_1}, \bar{d_2})$ as z tends to 0 but, depending on the values of δ, its shape may change. Approaching it by the lower-order terms, two cases appear.

For $\delta < 1$, we have

$$\begin{aligned}\begin{pmatrix} d_1 \\ d_2^2 \end{pmatrix} &\approx \begin{pmatrix} \bar{d_1} \\ \bar{d}_2^2 \end{pmatrix} - \left[x_0 + \frac{BC - AD}{C}\bar{Z}\right] \\ &\quad \times z^{\delta} h^{-\delta} \begin{pmatrix} a & b \\ c & d \end{pmatrix} \begin{pmatrix} \cos\left(\theta \log z + \phi\right) \\ \sin\left(\theta \log z + \phi\right) \end{pmatrix},\end{aligned}$$

up to order $o(z^{\delta})$. The first term of the right-hand side corresponds to the point $\bar{P}$ and the second one is a parameterization of a linearly deformed logarithmic spiral. Taking square roots of the second components of the vectors at both sides of the equation we get a parabolically deformed logarithmic spiral around $\bar{P}$.

For $\delta > 1$, Eq. (9) can be written as

$$\begin{pmatrix} d_1 \\ d_2^2 \end{pmatrix} \approx \begin{pmatrix} \bar{d_1} \\ \bar{d}_2^2 \end{pmatrix} + \frac{1}{C} z \bar{Z}^{\Delta} H^{-\Delta} \begin{pmatrix} \cos\left(\Theta \log \bar{Z} + \Phi\right) \\ \sin\left(\Theta \log \bar{Z} + \Phi\right) \end{pmatrix}$$

up to order $o(z)$. Taking square roots of the second components of the vectors at both sides of the equation we obtain a parabolic curve that reaches $\bar{P}$ for $z=0$ (if $\cos\left(\Theta\log\bar{Z}+\Phi\right)=0$, resp. $\sin\left(\Theta\log\bar{Z}+\Phi\right)=0$, then the curves are vertical, resp. horizontal, straight lines). If $C>0$ the curve points, as z tends to 0, to the region surrounded by the curve of homoclinic connections to Q_1, while if $C<0$ it points to the opposite direction.

The following theorem summarizes the previous results:

Theorem 2 *Let us consider a point $\bar{P}=(\bar{d_1},\bar{d_2})$ of the curve of homoclinic connections to Q_1, with $\bar{d_2}>0$, which corresponds to a value $Z=\bar{Z}$. By fixing this value in Eq. (8), a curve of principal periodic orbits, parameterized by z, is obtained:*

1. *For $\delta<1$ the curve is, up to order $o(z^\delta)$, a parabolically deformed logarithmic spiral which tends to $\bar{P}$ as z tends to 0.*
2. *For $\delta>1$ the curve is, up to order $o(z)$, a segment of a parabolic curve that tends to $\bar{P}$ as z tends to 0.*

For completing the study of the curves of periodic orbits close to the curves of homoclinic connections, it is necessary to make some remarks to this theorem.

The theorem describes the local shape of the curves. It is obvious that, as z increases, the higher order terms will change this shape, and oscillations may appear. This is the reason why there may be curves of saddle-node bifurcations of periodic orbits close to the T-point even in the case where $\delta>1$.

If the point $\bar{P}$ is chosen very close to $d_2=0$, then there are interactions between the obtained curve of periodic orbits and its symmetrical one. Thus, closed curves may appear near the curve of homoclinic connections. Moreover, if $\bar{P}$ is chosen with $d_2=0$, all the corresponding curves of periodic orbits in the vicinity of $\bar{P}$ will be closed.

If a value $Z=\bar{Z}$ is fixed in Eq. (2), the discriminant of the square root of Eq. (2) is negative for values of μ below a critical value μ_Z. This means that it does not correspond to any point of the curve of homoclinic connections to Q_1. Even in this case, if μ is close enough to μ_Z, there will exist a remainder of closed curves of periodic orbits that disappear as $\mu_Z-\mu$ increases.

3.2 Saddle-node bifurcations of principal periodic orbits

From now on, we are going to assume that the respective saddle indices of the equilibria verify $\delta<1$ and $\Delta<1$. That is, both equilibria satisfy Shil'nikov's condition.

In order to derive the equations for the saddle-node bifurcations of principal periodic orbits, let us define

$$\begin{aligned}\begin{pmatrix} M_1(z,Z;d_1,d_2,\mu)\\ M_2(z,Z;d_1,d_2,\mu)\end{pmatrix} &= -\begin{pmatrix} d_1\\ d_2^2-\mu\end{pmatrix}\\ &+[X_0+\frac{1}{C}(z-DZ)]Z^{\Delta}H^{-\Delta}\\ &\times\begin{pmatrix}\cos\left(\Theta\log Z+\Phi\right)\\ \sin\left(\Theta\log Z+\Phi\right)\end{pmatrix}\\ &-[x_0+\frac{1}{C}(Az+(BC-AD)Z)]z^{\delta}h^{-\delta}\\ &\times\begin{pmatrix} a & b\\ c & d\end{pmatrix}\begin{pmatrix}\cos\left(\theta\log z+\phi\right)\\ \sin\left(\theta\log z+\phi\right)\end{pmatrix}.\end{aligned} \tag{10}$$

Thus, the system of equations for the principal periodic orbits is

$$\begin{pmatrix} M_1(z,Z;d_1,d_2,\mu)\\ M_2(z,Z;d_1,d_2,\mu)\end{pmatrix}=\begin{pmatrix}0\\0\end{pmatrix}. \tag{11}$$

A saddle-node bifurcation for this system appears when (z,Z) cannot be uniquely determined as functions of (d_1,d_2,μ) from Eqs. (11). This means that the corresponding Jacobian vanishes:

$$\begin{aligned}J(z,Z) &= \det\begin{pmatrix} M_{1z} & M_{1Z}\\ M_{2z} & M_{2Z}\end{pmatrix}\\ &= M_{1z}M_{2Z}-M_{1Z}M_{2z}=0,\end{aligned} \tag{12}$$

where the subscripts z and Z stand for the corresponding partial derivatives. Note that Eq. (12) is only a necessary condition in order to have a saddle-node bifurcation.

Once the derivatives have been developed, Eq. (12) can be written as

$$\begin{aligned}0=J(z,Z) &= x_0X_0h^{-\delta}H^{-\Delta}z^{\delta-1}Z^{\Delta-1}\\ &\times[\vartheta_1\cos(\Theta\log Z+\Phi)\,\sin(\theta\log z+\phi)\\ &\quad+\vartheta_2\cos(\Theta\log Z+\Phi)\cos(\theta\log z+\phi)\\ &\quad+\vartheta_3\,\sin(\Theta\log Z+\Phi)\,\sin(\theta\log z+\phi)\\ &\quad+\vartheta_4\,\sin(\Theta\log Z+\Phi)\cos(\theta\log z+\phi)]+\cdots,\end{aligned} \tag{13}$$

where the dots stand for higher-order terms and

$$\begin{pmatrix}\vartheta_1\\ \vartheta_2\\ \vartheta_3\\ \vartheta_4\end{pmatrix}=\begin{pmatrix}-\theta\Theta & \delta\Theta & \Delta\theta & -\delta\Delta\\ \delta\Theta & \theta\Theta & -\delta\Delta & -\Delta\theta\\ -\Delta\theta & \delta\Delta & -\theta\Theta & \delta\Theta\\ \delta\Delta & \Delta\theta & \delta\Theta & \theta\Theta\end{pmatrix}\begin{pmatrix}a\\ b\\ c\\ d\end{pmatrix}.$$

Note that the coefficients ϑ_i, with $i=1,2,3,4$, are obtained as a nonsingular linear transformation of a, b, c and d, since

$$\det\begin{pmatrix}-\theta\Theta & \delta\Theta & \Delta\theta & -\delta\Delta\\ \delta\Theta & \theta\Theta & -\delta\Delta & -\Delta\theta\\ -\Delta\theta & \delta\Delta & -\theta\Theta & \delta\Theta\\ \delta\Delta & \Delta\theta & \delta\Theta & \theta\Theta\end{pmatrix}=(\delta^2+\theta^2)^2(\Delta^2+\Theta^2)^2\neq 0.$$

On the other side, the coefficients also verify

$$\vartheta_1\vartheta_4-\vartheta_2\vartheta_3=(\delta^2+\theta^2)(\Delta^2+\Theta^2)(bc-ad)\neq 0. \tag{14}$$

Therefore $\vartheta_1\vartheta_4 - \vartheta_2\vartheta_3$ and $bc - ad$ have the same sign.

An important remark is that Eq. (12) does not depend on the parameters (d_1, d_2, μ). Thus, we are going to study the existence of solutions of Eq.(12) in the plane of variables (z, Z).

The global bifurcations at the (z, Z)-plane have very easy locations: the T-point heteroclinic cycle is the origin and the homoclinic connections to Q_1 and Q_2 correspond, respectively, to $z = 0$, $Z > 0$ and to $Z = 0$, $z > 0$.

The solutions (z, Z) to Eq. (12), can be organized, depending on the sign of $\theta\Theta(ad - bc)$ in two kinds of curves which are now going to be described.

Solving Eq. (13) for z, we obtain

$$\begin{aligned} z = \exp\Bigg(\frac{1}{\theta}\bigg[\frac{\pi}{2} + l_1\pi - \phi \\ + \operatorname{arctg}\left(\frac{\vartheta_1 \cos(\Theta \log Z + \Phi) + \vartheta_3 \sin(\Theta \log Z + \Phi)}{\vartheta_2 \cos(\Theta \log Z + \Phi) + \vartheta_4 \sin(\Theta \log Z + \Phi)}\right)\bigg]\Bigg) \\ \times (1 + \cdots), \end{aligned} \tag{15}$$

where l_1 is any integer and the dots stand for terms that tend to zero as (z, Z) tends to $(0, 0)$.

Every integer value of l_1 determines, up to first order, a curve with discontinuities at

$$Z_{l_2} = \exp\left(\frac{1}{\Theta}\left[l_2\pi - \Phi - \operatorname{arctg}\left(\frac{\vartheta_2}{\vartheta_4}\right)\right]\right)$$

where $l_2 \in \mathbb{Z}$. Each part of such a curve among two consecutive discontinuities corresponds to an increasing or decreasing function (depending on the sign of $\theta\Theta(ad - bc)$) whose maximum and minimum values are given, respectively, by $z = \exp\left([(l_1 + 1)\pi - \phi]/\theta\right)$ and $z = \exp\left((l_1\pi - \phi)/\theta\right)$. Joining pieces of curves for consecutive values of l_1 it is possible to obtain continuous curves.

To be more precise, taking l_1 as a function of Z in the following way

$$\begin{aligned} l_1(Z) = m_1 + \operatorname{sg}(ad - bc) \\ \times \operatorname{INT}\left(\frac{1}{\pi}\left[\Theta \log Z + \Phi + \operatorname{arctg}\left(\frac{\vartheta_2}{\vartheta_4}\right)\right]\right), \end{aligned} \tag{16}$$

where $\operatorname{INT}(\cdot)$ stands for the integer part function and $m_1 \in \mathbb{Z}$, and substituting $l_1 = l_1(Z)$ in Eq. (15) we get, for every value of m_1, a continuous curve at the plane (z, Z) whose asymptotic expansion up to first order is given by

$$\begin{aligned} z = \exp\Bigg(\frac{1}{\theta}\bigg[\frac{\pi}{2} + l_1(Z)\pi - \phi \\ + \operatorname{arctg}\left(\frac{\vartheta_1 \cos(\Theta \log Z + \Phi) + \vartheta_3 \sin(\Theta \log Z + \Phi)}{\vartheta_2 \cos(\Theta \log Z + \Phi) + \vartheta_4 \sin(\Theta \log Z + \Phi)}\right)\bigg]\Bigg). \end{aligned} \tag{17}$$

Depending on the sign of $\theta\Theta(ad - bc)$ the curves given by Eq. (17) have different shapes: if $\theta\Theta(ad-bc) > 0$ then the curves tend to the origin (that is, to the T-point) as parabola-like (with oscillations) functions; if $\theta\Theta(ad - bc) < 0$ the curves pass from an axis to the other as hyperbola-like (with oscillations) functions. The following study has been performed assuming that $\theta\Theta(ad-bc) > 0$ because this is the case observed in the numerical analysis of Chua's equations [5].

To complete the analysis of saddle-node bifurcations of periodic orbits in the plane (z, Z) an important detail has to be taken into account: not every solution (z, Z) to Eq. (12) corresponds to a saddle-node bifurcation of periodic orbits because once a solution (z, Z) to Eq. (12) has been obtained, it has to be substituted into Eq. (8) for getting the corresponding values of the principal parameters and this can be done only if the second equation of (8) can be solved for d_2. That is, only if the function

$$\begin{aligned} \operatorname{disc}(z, Z; \mu) = \mu \\ + \left[X_0 + \frac{1}{C}(z - DZ)\right] Z^{\Delta} H^{-\Delta} \sin\left(\Theta \log Z + \Phi\right) \\ - \left[x_0 + \frac{1}{C}(Az + (BC - AD)Z)\right] z^{\delta} h^{-\delta} \\ \times \left(c \cos\left(\theta \log z + \phi\right) + d \sin\left(\theta \log z + \phi\right)\right), \end{aligned} \tag{18}$$

is not negative.

From now on we define the *admissible region for the parameter* μ to mean the subset of the (z, Z)-plane given by

$$\mathcal{AR}_\mu = \left\{(z, Z) \in \overline{\mathbb{R}^+ \times \mathbb{R}^+} \ : \ \operatorname{disc}(z, Z; \mu) \geq 0\right\}.$$

We define the *inadmissible region for the parameter* μ to mean the complementary subset,

$$\mathcal{IR}_\mu = \overline{\mathbb{R}^+ \times \mathbb{R}^+} \setminus \mathcal{AR}_\mu.$$

For each value of the parameter μ the equation

$$\operatorname{disc}(z, Z; \mu) = 0$$

determines limit curves of the (z, Z)-plane where $d_2 = 0$. Usually, a curve of saddle-node bifurcations of periodic orbits will cross some of these limit curves passing from $\mathcal{AR}_\mu$ to $\mathcal{IR}_\mu$, or vice versa. The parts of the curves of saddle-node bifurcations of periodic orbits belonging to $\mathcal{AR}_\mu$ give two curves at the plane of parameters (d_1, d_2) which are symmetric with respect to $d_2 = 0$. The points where the curves of saddle-node bifurcations of periodic orbits intersect the limit curves $\operatorname{disc}(z, Z; \mu) = 0$ will correspond to the connections between the symmetric curves at $d_2 = 0$.

Let us now analyze briefly the different regions $\mathcal{AR}_\mu$ and $\mathcal{IR}_\mu$ that can be obtained for the different values of μ.

If $\mu > 0$, the origin belongs to $\mathcal{AR}_\mu$; the function $\operatorname{disc}(z, Z; \mu)$ is positive for values of (z, Z) close to the origin while it can be negative for higher values of (z, Z). In order to separate roughly the origin and $\mathcal{IR}_\mu$, we can substitute the trigonometric functions of $\mathrm{disc}(z, Z; \mu)$ by their maximum values. The limit curve, in the (z, Z)-plane, of this approximation is given by

$$\begin{aligned}\mu = &\left[X_0 + \frac{1}{C}(z - DZ)\right] Z^{\Delta} H^{-\Delta} \\ &+ \left[x_0 + \frac{1}{C}(Az + (BC - AD)Z)\right] z^{\delta} h^{-\delta} \sqrt{c^2 + d^2}.\end{aligned} \tag{19}$$

Fixing $z = 0$ (the curve of homoclinic connections to Q_1 in the (z, Z)-plane) in Eq. (18), we obtain

$$\mu = -[X_0 - \frac{D}{C} Z] Z^{\Delta} H^{-\Delta} \sin(\Theta \log Z + \Phi). \tag{20}$$

The right-hand side is an oscillating function whose amplitude is bounded by

$$\mu = [X_0 - \frac{D}{C} Z] Z^{\Delta} H^{-\Delta}. \tag{21}$$

As Z is increased there is a value Z^* where Eq. (21) holds. Thus, the function given by Eq. (20) vanishes for a sequence of values greater than Z^*. This means that, over the curve of homoclinic connections to Q_1, there are intervals belonging to $\mathcal{IR}_\mu$ for $Z > Z^*$. For small values of μ, this phenomenon is close to the origin and can be considered as a consequence of the non-transversal T-point.

In a similar way, fixing $Z = 0$ (curve of homoclinic connections to Q_2 in the (z, Z)-plane) in Eq. (19) we obtain

$$\begin{aligned}\mu = &[x_0 + \frac{A}{C} z] z^{\delta} h^{-\delta} \\ &\times (c \cos(\theta \log z + \phi) + d \sin(\theta \log z + \phi)),\end{aligned} \tag{22}$$

which corresponds to an oscillating curve whose amplitude is bounded by

$$\mu = [x_0 + \frac{A}{C} z] z^{\delta} h^{-\delta} \sqrt{c^2 + d^2}. \tag{23}$$

For small values of μ, there is a value z^* where Eq. (23) holds and can be considered as a lower bound to the intervals of $Z = 0$ that belong to $\mathcal{IR}_\mu$.

If $\mu = 0$, the function $\mathrm{disc}(z, Z; 0)$ vanishes at the origin. Thus, due to the oscillating terms of Eq. (18), every neighbourhood of the origin intersects both regions $\mathcal{AR}_0$ and $\mathcal{IR}_0$.

For $\mu < 0$, the origin belongs to $\mathcal{IR}_\mu$; the function $\mathrm{disc}(z, Z; \mu)$ is negative for values of (z, Z) close to the origin while it is positive at some regions corresponding to higher values of (z, Z). Interchanging $\mathcal{IR}_\mu$ and $\mathcal{AR}_\mu$, the situation is similar to the positive case: a limit curve that separates the origin and $\mathcal{AR}_\mu$ can be obtained.

With the aim of showing these cases, we have fixed the following (arbitrary) values of the non-principal parameters of the theoretical model:

$$\begin{aligned}&a = 1,\ b = 2,\ c = 1,\ d = 1, \\ &A = -1,\ B = 1,\ C = -2,\ D = 1, \\ &p = 0.3,\ \lambda = 1,\ \omega = -5\pi, \\ &P = 0.7,\ \Lambda = 1,\ \Omega = -4\pi, \\ &x_0 = 0.01,\ X_0 = 0.01,\ h = 0.05,\ H = 0.05.\end{aligned} \tag{24}$$

These values have been chosen in order to verify the transversality condition between the two dimensional manifolds, $C \neq 0$, and to get an orientation-preserving Poincaré map. No additional restrictions have been assumed. Note that, with this election of the parameters, the values of the Shil'nikov constants of the two equilibria Q_1 and Q_2 are, respectively, $\delta = 0.3$ and $\Delta = 0.7$. Fixing now $\mu = 0.002$, $\mu = 0$ and $\mu = -0.002$, the three previous cases appear (see Fig. 4).

An important result is that there exists a relationship between the curves of saddle-node bifurcations in the (z, Z)-plane and the points where $\mathrm{disc}(z, Z; \mu)$ vanishes. As we have seen in Fig. 4, the sets $\mathcal{AR}_\mu$ and $\mathcal{IR}_\mu$ are organized as "islands" or "holes" that vary (growing, shrinking, merging,...) as μ changes. Concretely, as μ decreases, the points from which the different parts of $\mathcal{IR}_\mu$ emerge are local minima, the points where $\mathcal{AR}_\mu$ disappears are local maxima and the points where two "islands" or "holes" of $\mathcal{AR}_\mu$ or $\mathcal{IR}_\mu$ have a contact, correspond to saddle points of $\mathrm{disc}(z, Z; \mu)$. At stationary points of $\mathrm{disc}(z, Z; \mu)$ the gradient (M_{2z}, M_{2Z}) vanishes. Obviously, this implies that $J = 0$, and proves the following result:

Proposition 1 *In the plane of coordinates (z, Z), the stationary points of* $\mathrm{disc}(z, Z; \mu)$ *lie on curves of saddle-node bifurcations of periodic orbits.*

In the numerical analysis of the theoretical model, proposition 1 plays a very important role, because it allows the understanding of the complete mechanism of creation/destruction of closed curves of saddle-node bifurcations.

3.3 Cusp bifurcations

A necessary condition for the appearance of a cusp bifurcation of periodic orbits at a curve of saddle-node bifurcations of periodic orbits (see [15], [12]) is that the tangent vector of the curve vanishes. That is, consider a parameterized curve of saddle-node bifurcations of periodic orbits

$$(z, Z) = (z(s), Z(s)) \tag{25}$$

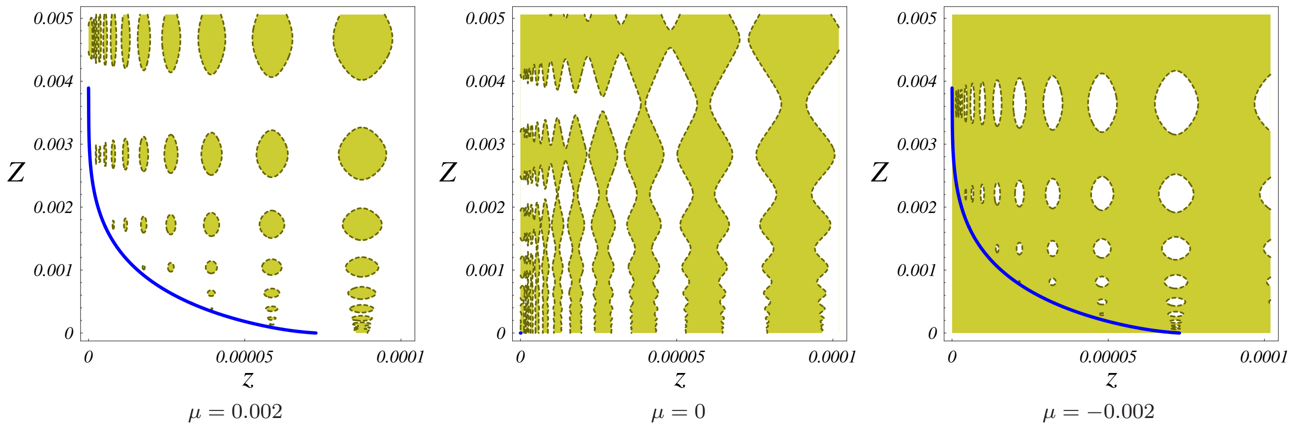

Fig. 4 Regions $\mathcal{AR}_\mu$ (white) and $\mathcal{IR}_\mu$ (shaded) in the (z, Z)-plane, obtained from the theoretical model for the values of the parameters given by (24). The three figures correspond to $\mu = 0.002$, $\mu = 0$ and $\mu = -0.002$. The limit curve given by (19) is shown for $\mu = 0.002$ and $\mu = -0.002$

and the corresponding curve at the parameter (d_1, d_2) plane

$$\begin{pmatrix} d_1 \\ d_2 \end{pmatrix} = \begin{pmatrix} d_1(z(s), Z(s)) \\ d_2(z(s), Z(s)) \end{pmatrix},$$

which is obtained from (8). The tangent vector of this curve vanishes if

$$\begin{cases} \dfrac{\partial d_1}{\partial z} z'(s) + \dfrac{\partial d_1}{\partial Z} Z'(s) = 0, \\ \dfrac{\partial d_2}{\partial z} z'(s) + \dfrac{\partial d_2}{\partial Z} Z'(s) = 0. \end{cases} \tag{26}$$

From Eqs. (8) and (10) it is obvious that the derivatives of d_1 and M_1, with respect to z and Z, coincide. In the case of d_2, using the notation (18), these derivatives are given by

$$2d_2(z, Z; \mu)\frac{\partial d_2}{\partial z}(z, Z; \mu) = \mathrm{disc}_z(z, Z; \mu),$$
$$2d_2(z, Z; \mu)\frac{\partial d_2}{\partial Z}(z, Z; \mu) = \mathrm{disc}_Z(z, Z; \mu).$$

As the derivatives of $\mathrm{disc}(z, Z; \mu)$ with respect to z and Z coincide with the corresponding derivatives of M_2, when $\mathrm{disc}(z, Z; \mu)$ does not vanish (that is, d_2 does not vanish), system (26) is equivalent to

$$\begin{cases} M_{1z} z'(s) + M_{1Z} Z'(s) = 0, \\ M_{2z} z'(s) + M_{2Z} Z'(s) = 0, \end{cases}$$

which means that both vectors (M_{1z}, M_{1Z}) and (M_{2z}, M_{2Z}) are orthogonal to $(z'(s), Z'(s))$.

Substituting Eq. (25) into the saddle-node equation (12) and taking derivatives with respect to the parameter s the following condition is obtained

$$J_z z'(s) + J_Z Z'(s) = 0.$$

Thus, vectors (J_z, J_Z), (M_{1z}, M_{1Z}) and (M_{2z}, M_{2Z}) are parallel in the case they do not vanish. In our analysis, this corresponds to the following set of conditions:

$$J = M_{1z}M_{2Z} - M_{1Z}M_{2z} = 0, \tag{27}$$
$$J_1 = J_Z M_{1z} - J_z M_{1Z} = 0, \tag{28}$$
$$J_2 = J_Z M_{2z} - J_z M_{2Z} = 0. \tag{29}$$

Note that condition (27), which is the necessary condition for saddle-node bifurcations given in Eq. (12), can be satisfied in two different ways. The non-trivial way is that (M_{1z}, M_{1Z}) and (M_{2z}, M_{2Z}) are non-zero parallel vectors. In this case, Eqs. (28) and (29) are equivalent. The trivial way to verify Eq. (27) is that one of the vectors, (M_{1z}, M_{1Z}) or (M_{2z}, M_{2Z}), vanishes.

The points where (M_{1z}, M_{1Z}) or (M_{2z}, M_{2Z}) are zero vectors correspond to special situations whose mathematical meaning is going to be remarked later. From now on, for the study of the generic case, we are going to assume that (M_{1z}, M_{1Z}) and (M_{2z}, M_{2Z}) do not vanish and, therefore, Eqs. (28) and (29) are equivalent. In that way, we study only Eq. (28).

Once the derivatives have been obtained, Eq. (28) can be written as

$$\begin{aligned}
&-x_0^2X_0h^{-2\delta}H^{-\Delta}z^{2\delta-2}Z^{\Delta-2}\\
&\quad\times[(a\delta+b\theta)\cos(\theta\log z+\phi)\\
&\qquad+(b\delta-a\theta)\sin(\theta\log z+\phi)]\\
&\quad\times[\vartheta_{13}\cos(\Theta\log Z+\Phi)\sin(\theta\log z+\phi)\\
&\qquad+\vartheta_{31}\sin(\Theta\log Z+\Phi)\sin(\theta\log z+\phi)\\
&\qquad+\vartheta_{24}\cos(\Theta\log Z+\Phi)\cos(\theta\log z+\phi)\\
&\qquad+\vartheta_{42}\sin(\Theta\log Z+\Phi)\cos(\theta\log z+\phi)]\\
&-x_0X_0^2h^{-\delta}H^{-2\Delta}z^{\delta-2}Z^{2\Delta-2}\\
&\quad\times[\Delta\cos(\Theta\log Z+\Phi)-\Theta\sin(\Theta\log Z+\Phi)]\\
&\quad\times[\vartheta_{12}\cos(\Theta\log Z+\Phi)\sin(\theta\log z+\phi)\\
&\qquad+\vartheta_{21}\cos(\Theta\log Z+\Phi)\cos(\theta\log z+\phi)\\
&\qquad+\vartheta_{34}\sin(\Theta\log Z+\Phi)\sin(\theta\log z+\phi)\\
&\qquad+\vartheta_{43}\sin(\Theta\log Z+\Phi)\cos(\theta\log z+\phi)]\\
&+\cdots=0,
\end{aligned}\tag{30}$$

where the dots stand for higher-order terms and the new coeficients are given by

$$\begin{pmatrix}\vartheta_{13}\\ \vartheta_{31}\\ \vartheta_{24}\\ \vartheta_{42}\end{pmatrix}=\begin{pmatrix}\Delta-1 & \Theta & 0 & 0\\ -\Theta & \Delta-1 & 0 & 0\\ 0 & 0 & \Delta-1 & \Theta\\ 0 & 0 & -\Theta & \Delta-1\end{pmatrix}\begin{pmatrix}\vartheta_1\\ \vartheta_3\\ \vartheta_2\\ \vartheta_4\end{pmatrix}$$

and

$$\begin{pmatrix}\vartheta_{12}\\ \vartheta_{21}\\ \vartheta_{34}\\ \vartheta_{43}\end{pmatrix}=\begin{pmatrix}\delta-1 & -\theta & 0 & 0\\ \theta & \delta-1 & 0 & 0\\ 0 & 0 & \delta-1 & -\theta\\ 0 & 0 & \theta & \delta-1\end{pmatrix}\begin{pmatrix}\vartheta_1\\ \vartheta_2\\ \vartheta_3\\ \vartheta_4\end{pmatrix}.$$

Note that both matrices are non-singular.

If we substitute the value of z given by equation (17) into (30), after some tedious algebra, it is possible to obtain an equivalent system, up to first order, to (27)-(28). This system is written in the following theorem:

Theorem 3 *If (M_{2z}, M_{2Z}) do not vanish then conditions (27)-(29) are equivalent, up to first order, to*

$$\begin{cases}X_0H^{-\Delta}(-1)^{l_1(Z)}\mathrm{sg}(\Psi_2)\left\|\begin{pmatrix}\Psi_1\\ \Psi_2\end{pmatrix}\right\|_2^3\theta Z^{\Delta}\\ \quad=-x_0h^{-\delta}\Theta(\delta^2+\theta^2)(ad-bc)(\vartheta_3\vartheta_2-\vartheta_1\vartheta_4)\\ \qquad\times\exp\left(\dfrac{\delta}{\theta}\left[\dfrac{\pi}{2}+l_1(Z)\pi-\phi+\mathrm{arctg}\left(\dfrac{\Psi_1}{\Psi_2}\right)\right]\right),\\ z=\exp\left(\dfrac{1}{\theta}\left[\dfrac{\pi}{2}+l_1(Z)\pi-\phi+\mathrm{arctg}\left(\dfrac{\Psi_1}{\Psi_2}\right)\right]\right),\end{cases}\tag{31}$$

where

$$\Psi_1=\vartheta_1\cos(\Theta\log Z+\Phi)+\vartheta_3\sin(\Theta\log Z+\Phi),$$
$$\Psi_2=\vartheta_2\cos(\Theta\log Z+\Phi)+\vartheta_4\sin(\Theta\log Z+\Phi),$$
$$l_1(Z)=m_1+\mathrm{sg}(ad-bc)\times\mathrm{INT}\left(\frac{1}{\pi}\left[\Theta\log Z+\Phi+\mathrm{arctg}\left(\frac{\vartheta_2}{\vartheta_4}\right)\right]\right)$$

and m_1 is any integer.

Let us remark that the first equation of system (31) does not depend on z. Thus, it can be solved for Z and then substituted into the second equation to obtain z.

On the other hand, if we compare the signs of the two sides of the first equation of (31) it is very easy to see that it can only have a solution for alternate values of m_1, because the right-hand term has a fixed sign for every integer m_1 while the sign of the left-hand term changes. Therefore, fixing a value of m_1 a curve of saddle-node bifurcations of periodic orbits is chosen in the plane of variables (z, Z) and if there exists a cusp bifurcation at one point of this curve then there are no cusp bifurcation points on the corresponding curves for m_1+1 and m_1-1.

Assuming that the value of m_1 verifies that the signs of both sides of the first equality of system (31) are the same, the existence of solutions to this equation can be proved by separately analysing both sides. The left-hand side corresponds to a power function of Z of exponent Δ, whose shape is modified by a bounded oscillatory function. The right-hand side corresponds to an oscillatory deformation of a power function of Z of exponent $\delta\Theta\mathrm{sg}(ad-bc)/\theta$. It is obvious that if both exponents are different, the equation will have at least one solution.

Note that the previous analysis is valid up to first order for values of (z, Z) close to the origin. It is trivial to extend it to the original equations having into account the higher-order terms. In this way we obtain the following existence theorem:

Theorem 4 *Assume that $\Delta\theta\neq\mathrm{sg}(ad-bc)\delta\Theta$ holds. Then, in a neighbourhood of the origin of the (z, Z)-plane, system (27)-(29) has solutions.*

Let us remark that for every fixed value of μ, a solution to system (27)-(29) corresponds to a pair of cusp bifurcations at the plane (d_1, d_2) provided that it belongs to the admissible region and that (M_{2z}, M_{2Z}) does not vanish.

Now, we are going to prove a relationship between tangencies, in the plane of coordinates (z, Z), of curves of saddle-node bifurcations of periodic orbits and solution curves to $\mathrm{disc}(z, Z;\mu)=0$ and collisions, in the plane of parameters (d_1, d_2), of symmetrical cusps bifurcations at points where $d_2=0$. This behaviour will be observed below, in the numerical analysis of the theoretical model, as a mechanism of creation/destruction of closed curves of saddle-node bifurcations.

As we know, stationary points of function $\mathrm{disc}(z, Z;\mu)$ appear for $(M_{2z}, M_{2Z})=(0,0)$. In this case, (27) and (29) hold, although (28) does not have to be satisfied. In other words, if an intersection point between a curve of saddle-node bifurcations and a solution curve to $\mathrm{disc}(z, Z; \mu) = 0$ is, at the same time, a stationary point of $\mathrm{disc}(z, Z; \mu)$, then it does not have to be a cusp point in the plane of parameters (d_1, d_2).

On the contrary, if a curve of saddle-node bifurcations and a solution curve to $\mathrm{disc}(z, Z; \mu) = 0$ have a non-transversal intersection which is not a stationary point of $\mathrm{disc}(z, Z; \mu)$, then it satisfies Eqs. (27)-(29), as the following proposition shows:

Proposition 2 *Let us assume that, in the (z, Z)-plane, a curve of saddle-node bifurcations of periodic orbits and a solution curve to* $\mathrm{disc}(z, Z; \mu) = 0$ *have a non-transversal intersection at a point $(z, Z) = (z_0, Z_0)$ for a certain value of μ. Let us assume that (z_0, Z_0) is not a stationary point of* $\mathrm{disc}(z, Z; \mu)$*. Then, Eqs. (27)-(29) hold.*

First, (27) holds because the intersection point belongs to the curve of saddle-node bifurcations. Second, at (z_0, Z_0), vectors (J_z, J_Z) and (M_{2z}, M_{2Z}) are, respectively, perpendicular to $J = 0$ and to $\mathrm{disc}(z, Z; \mu) = 0$. That is, at the tangency point they are parallel vectors and (29) holds. Third, as the intersection point is not a stationary point of $\mathrm{disc}(z, Z; \mu)$, (M_{2z}, M_{2Z}) does not vanish. Thus, condition (28) automatically holds because it is equivalent to (29). This finishes the proof of proposition 2.

The results given by proposition 2 can be transferred directly to the plane of parameters (d_1, d_2). On the one hand, a point which satisfies $\mathrm{disc}(z, Z; \mu) = 0$ is located at $d_2 = 0$ and, as we know, the full plane of parameters is symmetrical with respect to this axis. On the other hand, if this point also satisfies (27)-(29), it is, generically, a cusp bifurcation of periodic orbits (note that some additional degeneration conditions may give rise to more degenerate behaviours of codimension three or higher such as degenerate cusps and swallowtail bifurcations). Moreover, in the generical case, this cusp bifurcation will be located at $d_2 = 0$ and, due to the symmetry, there will be a pair of cusp bifurcations coexisting at that point.

Let us summarize the last results in the following theorem, whose proof is obvious from proposition 2:

Theorem 5 *Let us assume that, in the plane of coordinates (z, Z), a curve of saddle-node bifurcations of periodic orbits and a solution curve to* $\mathrm{disc}(z, Z; \mu) = 0$ *have a non-transversal intersection at a point $(z, Z) = (z_0, Z_0)$ for a certain value of μ. Let us assume that (z_0, Z_0) is not a stationary point of* $\mathrm{disc}(z, Z; \mu)$*. Then, generically, in the plane of parameters (d_1, d_2), two cusp bifurcations of periodic orbits, symmetrical with respect to $d_2 = 0$, collide at a point $(d_{10}, 0)$, where d_{10} is obtained substituting (z_0, Z_0) into equation (8).*

3.4 Numerical study of the model

To finish this study of the model, we are going to numerically analyze the curves of saddle-node bifurcations of periodic orbits given by (12) and, at the same time, we will compare the obtained results with the previously observed phenomena in Chua's equation [5]. The evolution of these curves, as a consequence of the failure of transversality of the T-points curve, will be shown (from the creation/destruction of closed curves, in two different ways, to the appearance of cusp bifurcations of periodic orbits).

This behaviour is analyzed by showing a sequence of figures corresponding to the plane of parameters (d_1, d_2) for different values of μ. To be precise, we fix a small positive value of μ and, while it decreases to reach negative values, several curves of bifurcations are analyzed.

Let us describe the procedure used for performing the numerical study. First, it is necessary to fix the values of the secondary parameters (namely, we take the values given in (24)).

Second, a region of the plane of coordinates (z, Z) (close to the origin) is selected. Several curves of saddle-node bifurcations of periodic orbits, solutions to (12), can be detected there. As we said previously, these curves do not change as μ varies, thus, they can be obtained by continuation and, then, used for every value of μ. The only difference is that, as μ decreases, the region $\mathcal{IR}_\mu$ grows. As a consequence of this, the curves of saddle-node bifurcations of periodic orbits disappear as μ decreases.

Third, the curves have to be represented in (d_1, d_2). In order to do this, we have to remove the intervals of the curves previously continued that lie within $\mathcal{IR}_\mu$. Then, the remaining parts of the curves are translated to the plane of parameters (d_1, d_2) by using equation (8).

The curves of saddle-node bifurcations of periodic orbits are organized, in the plane of coordinates (z, Z), as a sequence of parabola-like curves (with oscillations) that tends to the origin. These curves, once they are translated to the plane of parameters (d_1, d_2), may exhibit cusp bifurcations. Usually, depending on the values of the parameters, the cusp bifurcations appear only when the curves of saddle-node bifurcations of periodic orbits pass through a concrete region of the plane (z, Z). This region can be understood as the limit between the zone where periodic orbits are related to the homoclinic connections of Q_1 and the zone where they correspond to Q_2.

The relative locations of the curves of saddle-node bifurcations in the plane (z, Z), with respect to the curves of homoclinic connections, can be easily trans-

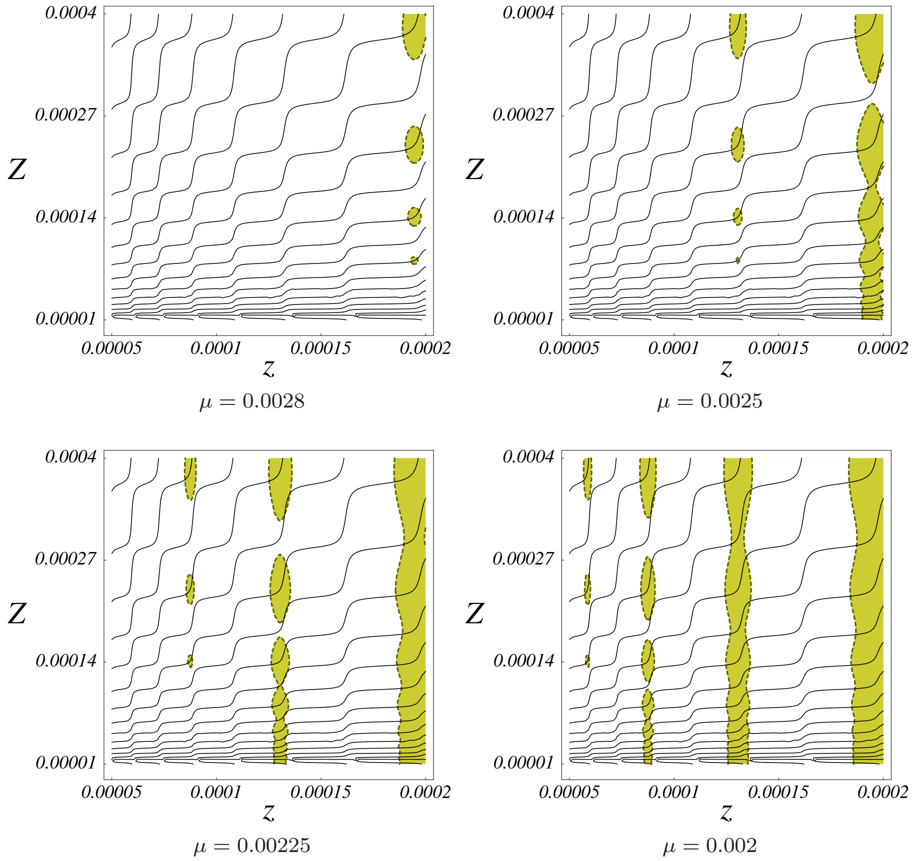

Fig. 5 Appearance of new subsets of $\mathcal{IR}_\mu$, in the plane of coordinates (z, Z), as μ tends to 0 taking positive values

lated into the plane (d_1, d_2). For example, the closer a curve is to the axis $z = 0$, the closer it is to the curve of homoclinic connections to Q_1 in the plane of parameters (d_1, d_2). Moreover, consecutive curves of the plane of coordinates (z, Z) are located at both sides of the curve of homoclinic connections in the plane (d_1, d_2), as in [15], dividing the set of curves in two kinds depending on the side of the curve of homoclinic connections where they are. In such a way, a curve of the plane (z, Z) surrounds, in the plane (d_1, d_2), every curve of the same kind which is closer to the axis $z = 0$. The same ideas are valid for the curves of saddle-node bifurcations near the curve of homoclinic connections to Q_2.

The curves of saddle-node bifurcations are, in the plane of parameters (d_1, d_2), spiral-like curves whose shapes remember of the shape of the curve of homoclinic connections to one of the equilibria. Let us assume that it corresponds to Q_1. As every spiral surrounds infinitely many other spirals of the same kind, there lays a spire of every other curve in the region bounded by two consecutive spires of a curve of saddle-node bifurcations. This explains that, between a contact of one of the spires of a curve with the axis $d_2 = 0$ and the contact of the next spire of the same curve with the same axis, the rest of the curves also have to touch this axis.

In Fig. 5, we can see this phenomenon as it can be observed in the plane of coordinates (z, Z), for curves whose shape is similar to the curve of homoclinic connections to Q_1. A contact between a curve of saddle-node bifurcations with $d_2 = 0$ corresponds, in the plane (z, Z), to an intersection between a solution curve to $J = 0$ and a solution curve to $\mathrm{disc}(z, Z; \mu) = 0$. As μ decreases, new subsets of $\mathcal{IR}_\mu$ appear: this means that new contacts between curves of saddle-node bifurcations and $d_2 = 0$ occur in the plane (d_1, d_2). The appearance of these subsets is arranged in the following way: they appear vertically for values of Z that tend to 0 as μ decreases and, once every curve has been intersected, new subsets appear vertically for a small value of z. This procedure is repeated once and again, infinitely many times, until $\mu = 0$ is reached. Note that the same phenomenon can be observed for curves close to the curve of homoclinic connections to Q_2 although, in this case, the order will be from right to left and from top to bottom.

Due to all these previous reasonings, to perform the numerical study, only two consecutive curves (in the

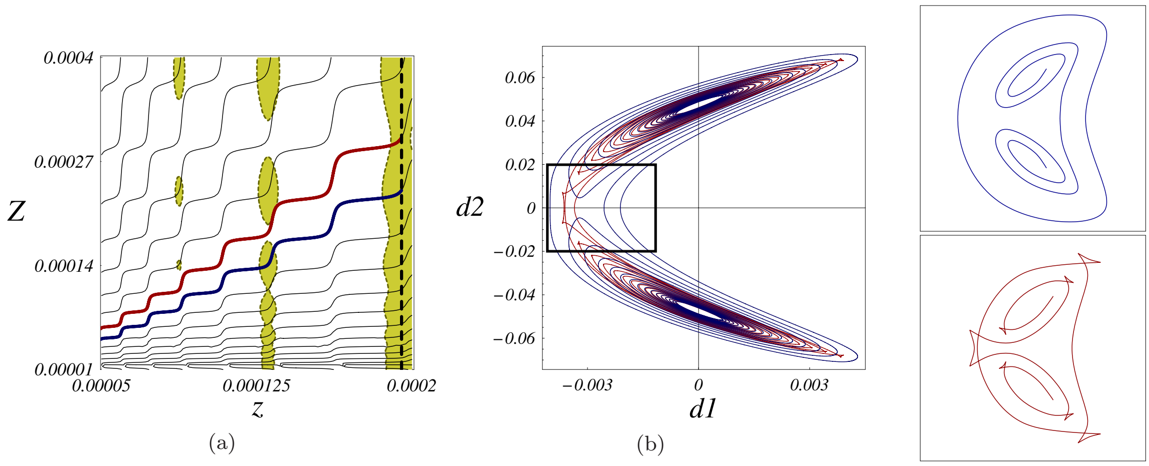

(a) (b) (c)

Fig. 6 For $\mu = 0.00226$ and the values of the parameters given by (24): (a) Detail of the curves of saddle-node bifurcations of periodic orbits at the region of the plane of coordinates (z, Z) where the numerical analysis is performed. Two of them (thicker curves) are selected. The region $\mathcal{IR}_\mu$ (shaded) is also shown. (b) The selected curves of saddle-node bifurcations of periodic orbits at the plane of parameters (d_1, d_2). (c) A schematic drawing of the two pairs of curves (with and without cusp bifurcations) that appear in (b)

plane of coordinates (z, Z)) are selected. They have been obtained, by using continuation, in a region where one of them exhibits cusp bifurcations. In figure 6(a), we show, for $\mu = 0.00226$, the curves of saddle-node bifurcations of periodic orbits at the region of the plane of coordinates (z, Z) where the numerical analysis is performed. The selected curves are thicker, the value where the continuation process is begun is shown as a dashed line and the set $\mathcal{IR}_\mu$ is shadowed. Figure 6(b) is obtained by translating both curves to the plane of parameters (d_1, d_2). Note that the selected pair of curves of the plane (z, Z) gives rise to four curves in the plane of parameters (d_1, d_2). Two of them are closed curves which correspond to the parts of the curves of the plane (z, Z) contained by $\mathcal{AR}_\mu$ and delimited by two consecutive intersections with $\mathrm{disc}(z, Z; \mu) = 0$ (more or less, for values of z between 0.00013 and 0.00019). The other two curves are bi-spiraling curves around the two symmetrical T-points and they correspond, in the plane of coordinates (z, Z), to the parts of the selected curves that tends to the origin.

To better understand the phenomena of creation/destruction of bifurcation curves we cannot analyze a region of the plane of coordinates (z, Z) as big as the one shown in figure 6(a). On the contrary, we are going to present smaller areas around the interesting phenomena and only the curve whose shape changes structurally. In the same way, to avoid the appearance of a lot of different curves, we only consider a small area of the plane of parameters (d_1, d_2).

Let us begin with the evolution of a curve without cusp bifurcations (which is simpler to analyze). In Fig. 7, we show the transition from $\mu = 0.00224$ to $\mu = 0.0022386$. For the first value, the selected region of the plane of coordinates (z, Z) is fully contained within the set $\mathcal{AR}_\mu$. At the plane of parameters (d_1, d_2) there is a symmetrical double-spiral curve. One of the loops of the spiral (together with its symmetrical one) is passing very close to the $d_2 = 0$ axis. For the second value, a small "island" of $\mathcal{IR}_\mu$ intersects the curve of saddle-node bifurcations in the plane (z, Z). The corresponding effect at the plane of parameters (d_1, d_2) is the division of the previous curve in two parts: a closed curve and the rest of the symmetrical double-spiral curve (this transition corresponds to that shown in figure 5 of [5]). This mechanism of creation of closed curves is analogous to the case of curves of homoclinic connections [2].

Note that, from Fig. 7 and as a direct consequence of proposition 1, the points from which $\mathcal{IR}_\mu$ emerges, lie on the curve of saddle-node bifurcations. Thus, the appearance of a new "island" of $\mathcal{IR}_\mu$ implies the creation of a new closed curve of saddle-node bifurcations in the plane of parameters (d_1, d_2).

Now, we are going to briefly describe the mechanism of creation/destruction of closed curves of saddle-node bifurcations in the presence of cusps. Thus, we consider again the small piece of $\mathcal{IR}_\mu$, which grows as μ decreases. In this way, it will intersect the next curve of saddle-node bifurcations as it is shown in Fig. 8 for the values $\mu = 0.00205$ (no intersection), $\mu = 0.002025$ (tangency) and $\mu = 0.002$ (two intersections). As a consequence of this process, a new closed curve appears in the plane of parameters (d_1, d_2) but, in this case, in-

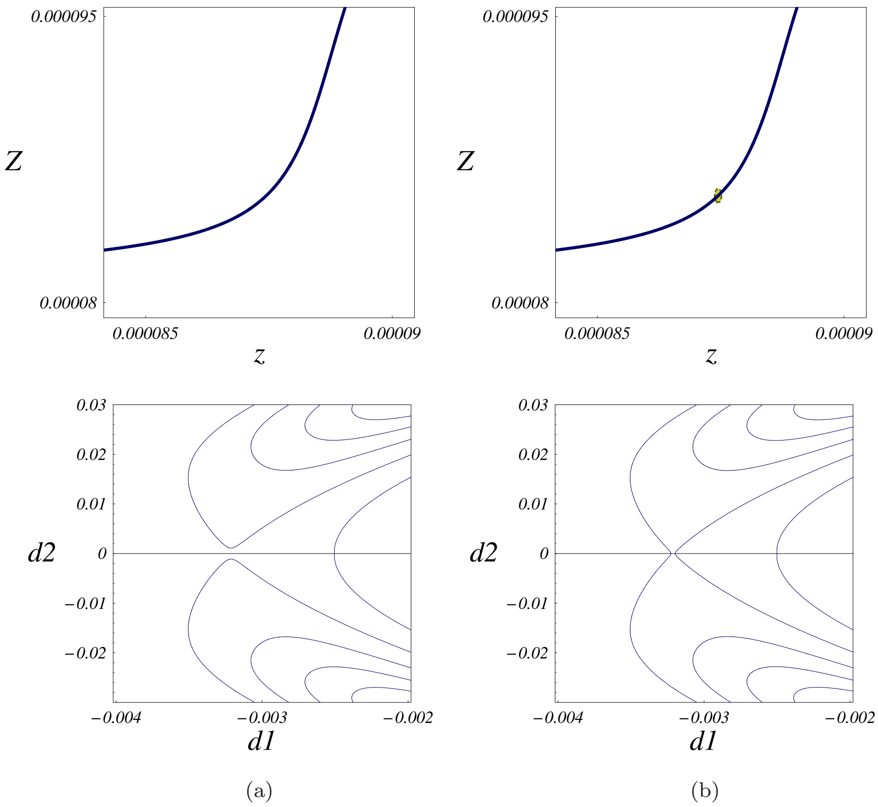

Fig. 7 For positive values of μ, (a) $\mu = 0.00224$, (b) $\mu = 0.0022386$: creation of a closed curve of saddle-node bifurcations for curves without cusp bifurcations

volving a collision between two symmetrical cusp bifurcations (see Theorem 5). This transition corresponds to that shown in figures 5(f) and 7(c) of [5].

Following the sequence, while the "island" of $\mathcal{IR}_\mu$ increases in size, it will merge with other subsets of $\mathcal{IR}_\mu$. This union occurs, in a saddle point, approximately for $\mu = 0.001988058$ (see Fig. 9). From it, a new closed curve appears in the plane of parameters (d_1, d_2). In this case the curve is smaller and it has two cusp bifurcations. The mechanism of its disappearance, a new tangency with the curve of saddle-node bifurcations, is illustrated with the other values, $\mu = 0.001987$ and $\mu = 0.0019815$. This transition corresponds to that shown in figure 7 of [5].

This is the complete evolution process that the curves of saddle-node bifurcations of periodic orbits exhibit as μ decreases, taking positive values. This mechanism is repeated once and again over the curve for smaller values of (z, Z) as μ tends to 0. Thus, for $\mu = 0$, each curve of the plane of coordinates (z, Z) gives infinitely many closed curves in the plane of parameters (d_1, d_2).

For negative values of μ, the curves gradually disappear. This mechanism is partially shown in Fig. 10 in the case of curves with cusps, although, in the plane of parameters (d_1, d_2) a closed curve without cusps is also represented for every value of μ. Let us begin with $\mu = -0.00208$. Firstly, due to the collision between two symmetrical cusps related to a tangency in the plane of coordinates (z, Z) (approximately at $\mu = -0.002093$), a small closed curve is created (for $\mu = -0.002097$ in Fig. 10) in the plane of parameters (d_1, d_2). Secondly, as μ decreases, the curve becomes smaller until it vanishes, corresponding to a saddle-point in the plane of coordinates (z, Z) (approximately for $\mu = -0.00209872$). Thirdly, the other closed curve disappears when a new tangency occurs in the plane of coordinates (z, Z). This last situation is not shown in Fig. 10.

The previous transition corresponds to that shown in figure 8 of [5].

The mechanism of destruction of curves without cusps has not been illustrated because it is very simple: curves disappear because they become smaller until they vanishes. This disappearance occurs for maximum points of $\mathrm{disc}(z, Z; \mu)$.

3.5 Another approach: singularity theory

Once the equations for saddle-node bifurcations of periodic orbits have been obtained, the core of our problem

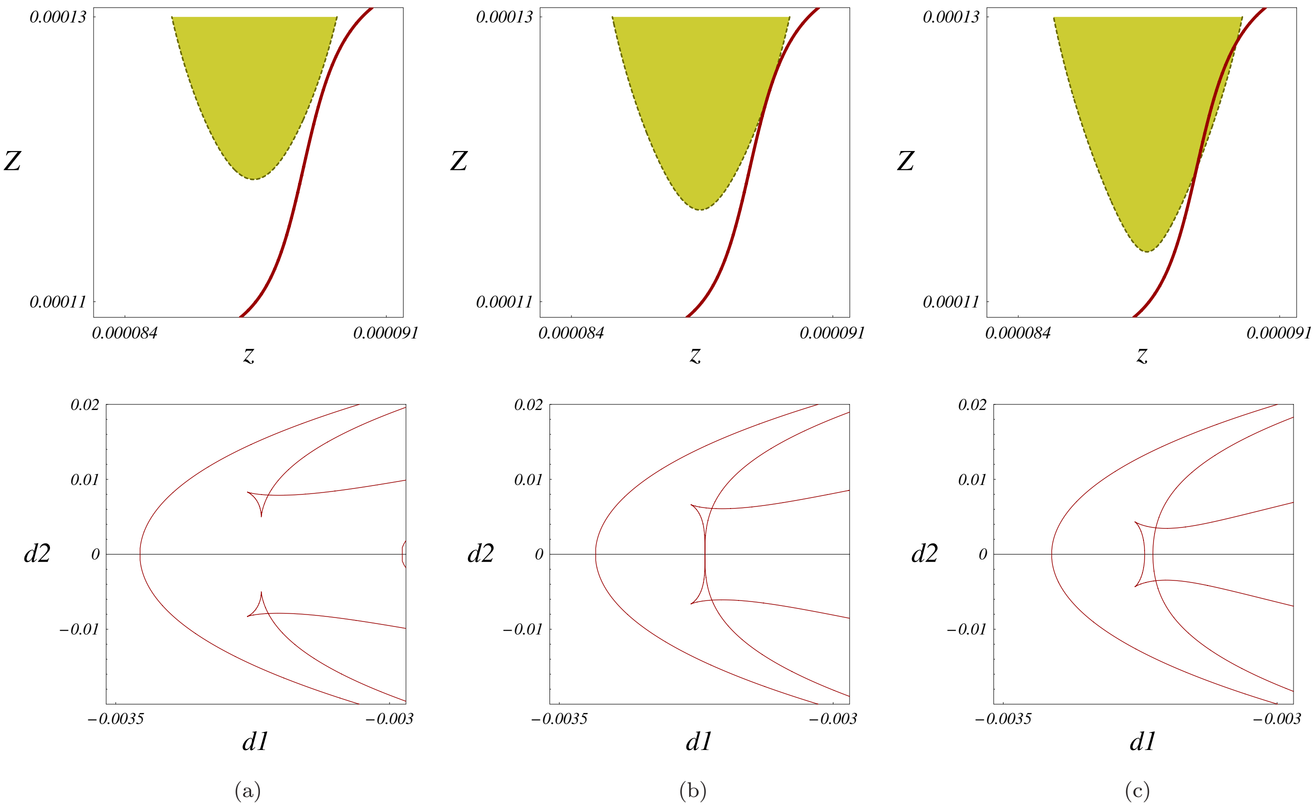

Fig. 8 For positive values of μ, (a) $\mu = 0.00205$, (b) $\mu = 0.002025$, (c) $\mu = 0.002$: creation (by a collision between two symmetrical cusp bifurcations) of a closed curve of saddle-node bifurcations for curves with cusp bifurcations

is simply to study the shape of the solution surfaces in the parameter space and their intersections with a sequence of planar sections corresponding to fixed values of the parameter μ. So, the original problem of finding and describing the dynamics organized by a non-transversal T-point is reduced to the problem of analyzing the solutions of several algebraic equations. From this point of view, singularity theory [6,7,17,29] can help us to understand some of the observed phenomena.

As an example of the use of singularity theory for a deeper comprehension of the structures shown in Sect. 3.4, we are going to give normal forms for the local transitions (involving intersections and tangencies between curves) shown in Figs. 8-10.

Let us begin with the generical manifold corresponding to the swallowtail catastrophe

$$H(x, A, B, C) \stackrel{\text{def}}{=} x^4 + Ax^2 + Bx + C = 0, \qquad (32)$$

and let us choose suitable values of (A, B, C) in terms of a new set of parameters (α, β, γ) to reproduce the behaviour observed in Figs. 8 and 9. The role of new parameters α, β and γ is similar to that of the principal parameters of the model d_1, d_2 and μ, respectively. That is, several values of γ will be fixed and the set of critical points of $H = 0$ (that is, points that satisfy $H_x = 0$) will be represented in (α, β) parameter plane.

Firstly, we fix $A = -1$ in order to have cusps in the curve of critical points. Secondly, we take $B = \beta^2 - \gamma - \alpha$ and $C = \beta^2 - \gamma + \alpha$. This choice can be easily explained in two steps: (α, β) parameters are mapped to $(\alpha, \beta^2 - \gamma)$ to get a duplicity effect for positive and negative values of β (that is, a symmetry with respect to $\beta = 0$) and a non-transversality for $\gamma = 0$; after that, they are rotated by 45 degrees with respect to the origin to get $(\beta^2 - \gamma - \alpha, \beta^2 - \gamma + \alpha)$, where the common factor $1/\sqrt{2}$ has been removed. Therefore, the manifold given by (32) can be written as

$$x^4 - x^2 + (\beta^2 - \gamma - \alpha)x + (\beta^2 - \gamma + \alpha) = 0. \qquad (33)$$

A sequence of planar slices of the set of critical points of manifold (33) for several values of γ is shown in Fig. 11. The curve configurations are almost exact to that shown in Figs. 8 and 9. The first contact between cusp points (shown in Fig. 11(b)) occurs for $\gamma = \frac{1}{72}\left(3 + 8\sqrt{6}\right)$ while the second one (where the small isola shown in Fig. 11(f) disappears) occurs for $\gamma = \frac{1}{72}\left(3 - 8\sqrt{6}\right)$.

Following similar ideas, if we take now $A = -1$, $B = -\beta^2 + \gamma + \alpha$ and $C = -\beta^2 + \gamma - \alpha$ (where the only

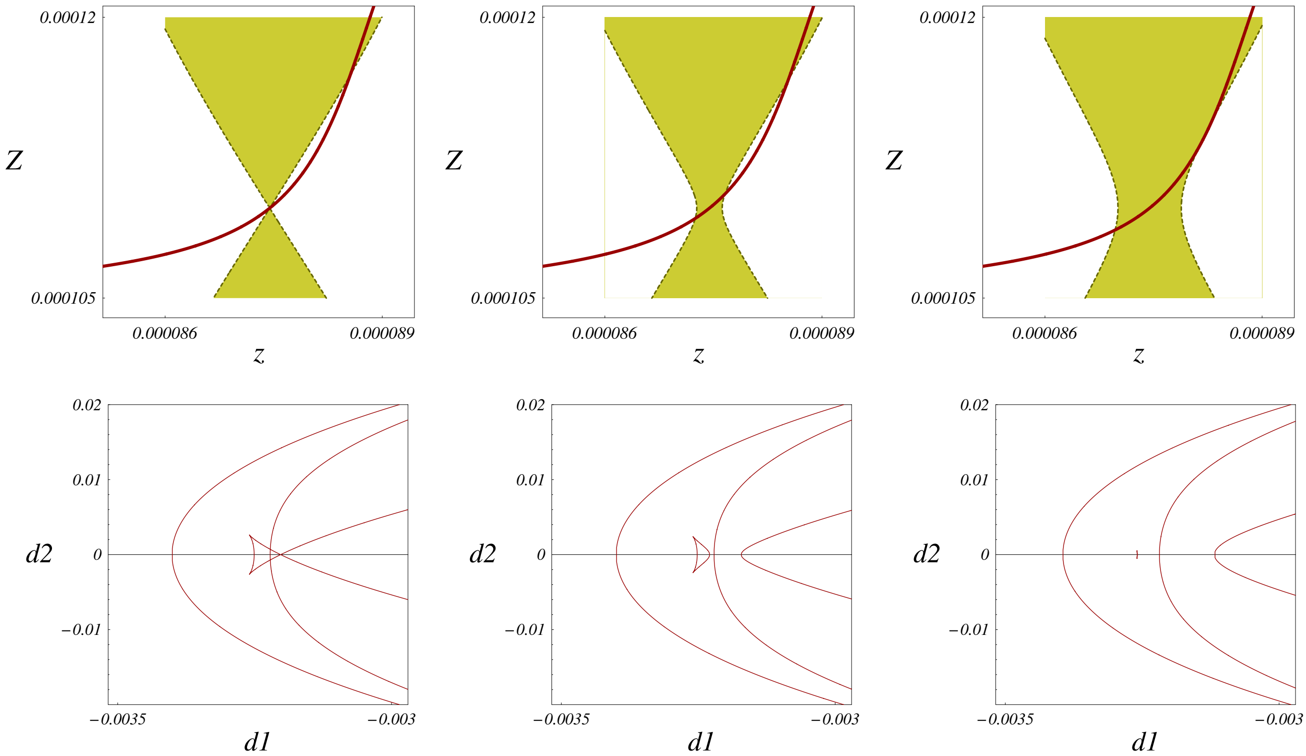

(a) (b) (c)

Fig. 9 For positive values of μ, (a) $\mu = 0.001988058$, (b) $\mu = 0.001987$, (c) $\mu = 0.0019815$: creation (by a non-transversal contact without cusps) and destruction (in an isola centre) of a closed curve of saddle-node bifurcations for curves with cusp bifurcations

difference is the rotation angle) the manifold given by (32) can be written as

$$x^4 - x^2 + (-\beta^2 + \gamma + \alpha)x + (-\beta^2 + \gamma - \alpha) = 0 \qquad (34)$$

and a new sequence of planar slices of the set of critical points can be obtained for several values of γ (compare Figs. 12 and 10). The first contact between cusp points (shown in Fig. 12(b)) occurs for $\gamma = \frac{1}{72}\left(-3 + 8\sqrt{6}\right)$ while the second one (where the small isola shown in Fig. 12(f) disappears) occurs for $\gamma = \frac{1}{72}\left(-3 - 8\sqrt{6}\right)$.

As we have just seen with these two examples, it is clear that the observed transitions (curves crossing, isola centres, cusps merging, ...) are principally due to the non-transversality of certain surfaces with respect to one distinguished parameter and, from this point of view, this behaviour can be expected from singularity theory (see, for instance, [6,7,17,29]). In fact, singularity theory may explain the way these bifurcations disappear when they interact with the non-transversality or even predict the appearance of swallowtail bifurcations. However, it is also clear that generically the existence of these cusp bifurcations is independent of the mentioned non-transversality.

In particular, the existence of cusp bifurcations of periodic orbits in the model is a direct consequence of the existence of the T-point (see Theorems 3 and 4) and it has nothing to do with the failure of transversality. Moreover, a deeper analysis of equation (31) shows that the cusp bifurcations must be confined to a region in the first quadrant of the (z, Z)-plane. So, a bad choice of the curve of saddle-node bifurcations or of the region where it is studied will not show any cusp bifurcation nor, obviously, the complicated transitions they exhibit close to the non-transversality.

4 Conclusions

Closed curves in bifurcation diagrams (isolas) or in bifurcation sets usually indicate the presence of a higher codimension bifurcation. Several examples have been found in the literature corresponding to bifurcations of periodic orbits.

The problem we consider is of interest because non-transversal T-points have been found in problems from many different fields: electronic circuits, pendula and laser problems [2,4,20,22,23,30].

The presence of closed curves of global bifurcations of periodic orbits has been numerically detected in Chua's equation [5].

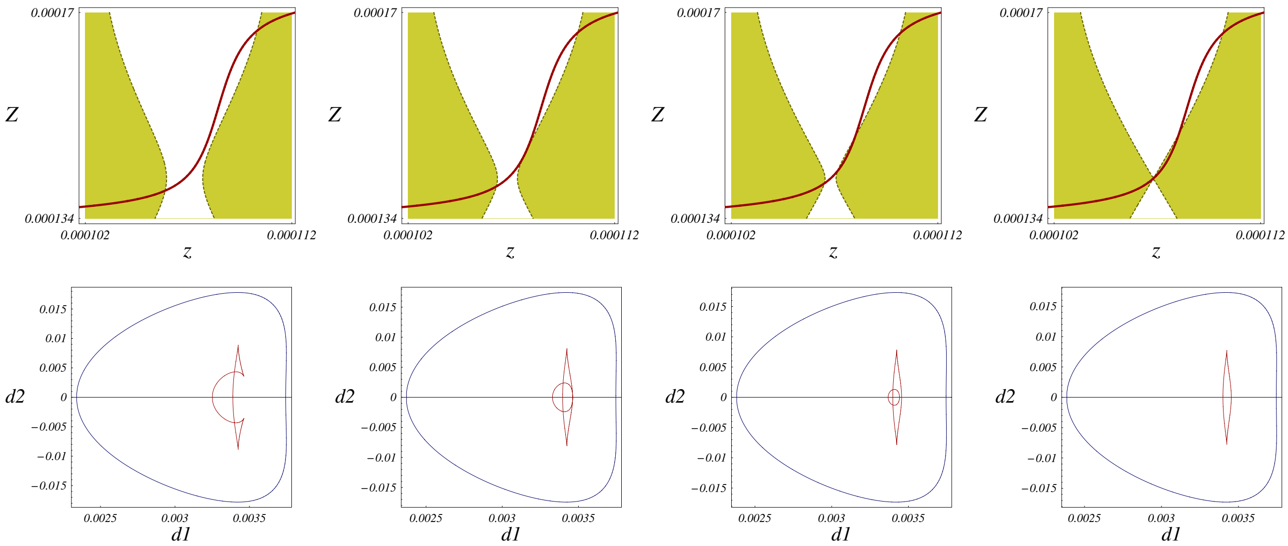

(a) (b) (c) (d)

Fig. 10 For negative values of μ, (a) $\mu = -0.00208$, (b) $\mu = -0.002093$, (c) $\mu = -0.002097$, (d) $\mu = -0.00209872$: creation (by a collision between two symmetrical cusp bifurcations) and destruction (in an isola centre) of a closed curve of saddle-node bifurcations for curves with cusp bifurcations. The bigger curve is of saddle-node bifurcations without cusps. The pair of curves, in the plane (d_1, d_2), that still appear in (d), disappear in two isola centres for smaller values of μ.

In the present work, we have studied a theoretical model that is able to find and describe the mechanism of the formation/destruction of such closed curves, relating them to a failure of transversality in a curve of T-points in a three-dimensional parameter space. In fact, we have shown that the appearance of closed curves of saddle-node bifurcations of periodic orbits and cusp bifurcations in the transition open-closed of some of them in a parameter plane may be caused by the presence of a nontransversality in the curve of T-points (if the equilibria involved are saddle-foci) in a three-dimensional parameter space.

We remark the good agreement between the predictions of the model and the curves numerically found in Chua's equation [5]. The model studied is able to account for the complex behaviour of the curves of saddle-node bifurcations (with and without cusps) previously found [5].

References

1. Algaba, A., Merino, M., Rodríguez-Luis, A. J.: Takens-Bogdanov bifurcations of periodic orbits and Arnold's tongues in a three-dimensional electronic model. Int. J. Bifurcation Chaos Appl. Sci. Eng. **11**, 513–531 (2001)
2. Algaba, A., Fernández–Sánchez, F., Freire, E., Merino, M., Rodríguez-Luis, A. J.: Nontransversal curves of T-points: a source of closed curves of global bifurcations. Phys. Lett. A **303**, 204–211 (2002)
3. Algaba, A., Merino, M., Freire, E., Gamero, E., Rodríguez-Luis, A. J.: Some results on Chua's equation near a triple-zero linear degeneracy. Int. J. Bifurcation Chaos Appl. Sci. Eng. **13**, 583-608 (2003)
4. Algaba, A., Merino, M., Fernández–Sánchez, F., Rodríguez-Luis, A. J.: Closed curves of global bifurcations in Chua's equation: a mechanism for their formation. Int. J. Bifurcation Chaos Appl. Sci. Eng. **13**, 609–616 (2003)
5. Algaba, A., Merino, M., Fernández–Sánchez, F., Rodríguez-Luis, A. J.: Open-to-closed curves of saddle-node bifurcations of periodic orbits near a nontransversal T-point in Chua's equation. Int. J. Bifurcation Chaos Appl. Sci. Eng. **16**, 2637–2647 (2006)
6. Arnold, V. I.: Singularity Theory. London Mathematical Society. Lecture Note Series 53. Cambridge University Press, Cambridge (1981)
7. Arrowsmith, D. K., Place, C. M.: An introduction to Dynamical Systems. Cambridge University Press, Cambridge (1994)
8. Bykov, V. V.: The bifurcations of separatrix contours and chaos. Physica D **62**, 290–299 (1993)
9. Champneys, A. R, Kirk, V., Knobloch, E., Oldeman, B. E., and Rademacher, J. D. M.: Unfolding a tangent equilibrium-to-periodic heteroclinic cycle'. SIAM J. Appl. Dyn. Syst. **8**, 1261-1304 (2009)
10. Champneys, A. R., Rodríguez-Luis, A. J.: The non-transverse Shil'nikov-Hopf bifurcation; uncoupling of homoclinic orbits and homoclinic tangencies. Physica D **128**, 130–158 (1999)
11. Doedel, E. J., Keller, H. B., Kernévez, J. P.: Numerical analysis and control of bifurcation problems (I) Bifurcation in finite dimensions. Int. J. Bifurcation Chaos Appl. Sci. Eng. **1**, 493–520 (1991)
12. Fernández–Sánchez, F.: Comportamiento dinámico y de bifurcaciones en algunas conexiones globales de equilibrios en sistemas tridimensionales (PhD Thesis)(2002)
13. Fernández–Sánchez, F., Freire, E., Rodríguez–Luis, A. J.: Isolas, cusps and global bifurcations in an electronic oscillator. Dyn. Stab. Syst. **12**, 319–336 (1997)

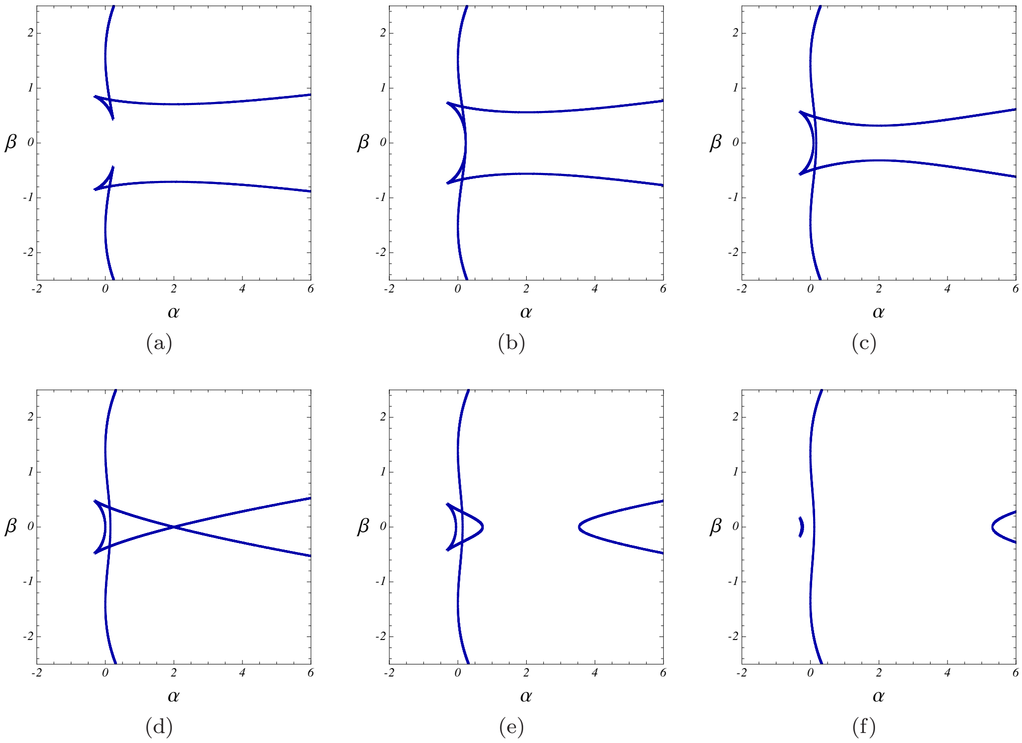

Fig. 11 Critical points of $x^4 - x^2 + (\beta^2 - \gamma - \alpha)x + (\beta^2 - \gamma + \alpha) = 0$ for (a) $\gamma = 0.5$, (b) $\gamma = \frac{1}{72}\left(3 + 8\sqrt{6}\right) \approx 0.31$, (c) $\gamma = 0.1$, (d) $\gamma = 0$, (e) $\gamma = -0.05$, (f) $\gamma = -0.2$.

14. Fernández–Sánchez, F., E. Freire, E., Rodríguez–Luis, A. J.: T-points in a $\mathbb{Z}_2$-symmetric electronic oscillator. (I) Analysis. Nonlinear Dyn. **28**, 53–69 (2002)
15. Gaspard, P., Kapral, R., Nicolis, G.: Bifurcation phenomena near homoclinic systems: a two-parameter analysis. J. Stat. Phys.**35**, 697–727 (1984)
16. Glendinning, P., Sparrow, C.: T-points: A codimension two heteroclinic bifurcation. J. Stat. Phys. **43**, 479–488 (1986)
17. Golubitsky, M., Schaeffer, D. G.: Singularities and Groups in Bifurcation Theory, Vol. I. Springer, Berlin (1985)
18. Guckenheimer, J., Holmes, P. J.: Nonlinear Oscillations, Dynamical Systems, and Bifurcations of Vector Fields. Springer, New York (1983)
19. Hirschberg, P., Laing, C.: Sucessive homoclinic tangencies to a limit cycle. Physica D **89**, 1–14 (1995)
20. Homburg, A., Natiello, M. A.: Accumulations of T-points in a model for solitary pulses in an excitable reaction-diffusion medium. Physica D **201**, 212–229 (2005)
21. Knobloch, J., Lamb, J.S.W., Webster, K.N.: Shift dynamics near T-point heteroclinic cycles. Preprint (2007)
22. Krauskopf, B., Oldeman B.: Bifurcation of global reinjection orbits near a saddle-node Hopf bifurcation. Nonlinearity **19**, 2149–2167 (2006)
23. Krauskopf, B., Sieber, J.: Bifurcation analysis of an inverted pendulum with delayed feedback control near a triple-zero eigenvalue singularity. Nonlinearity **17**, 85–103 (2004)
24. Kuznetsov, Yu.: Elements of Applied Bifurcation Theory. Springer, New York (2004)
25. Lamb, J.S.W., Teixeira, M.A., Webster, K.: Heteroclinic cycle bifurcations near Hopf-zero bifurcation in reversible vector fields in R^3. J. Differential Equations **219**, 78–115 (2005)
26. Lin, X. B.: Using Melnikov's method to solve Shilnikov's problems. Proc. Roy. Soc. Edinburgh **116 A**, 295–325 (1990)
27. Nayfeh, A. H., Balachandran, B.: Applied Nonlinear Dynamics. John Wiley & Sons, New York (1995)
28. Pivka, L., Wu, C. W., Huang, A.: Lorenz equation and Chua's equation. Int. J. Bifurcation Chaos Appl. Sci. Eng. **6**, 2443–2489 (1996)
29. Thom, R.: Structural stability and morphogenesis. The Benjamin/Cummings Publishing Company Inc., Reading, MA (1980)
30. Wieczorek, S., Krauskopf, B.: Bifurcations of n-homoclinic orbits in optically injected lasers. Nonlinearity **18**, 1095–1120 (2005)
31. Wiggins, S.: Introduction to Applied Dynamical Systems and Chaos. Springer, New York (2003)

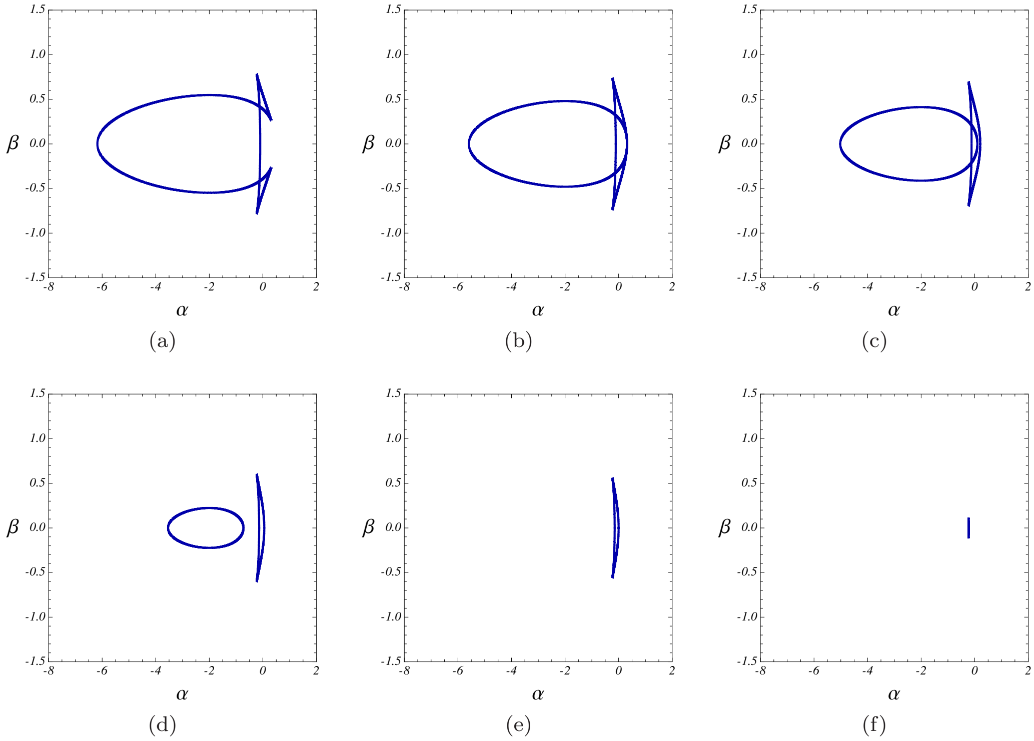

Fig. 12 Critical points of $x^4 - x^2 + (-\beta^2 + \gamma + \alpha)x + (-\beta^2 + \gamma - \alpha) = 0$ for (a) $\gamma = 0.3$, (b) $\gamma = \frac{1}{72}\left(-3 + 8\sqrt{6}\right) \approx 0.23$, (c) $\gamma = 0.17$, (d) $\gamma = 0.05$, (e) $\gamma = 0$, (f) $\gamma = -0.3$.